

Tailoring the flow of soft glasses by soft additives

E. Zaccarelli,^{1,2} C. Mayer,³ A. Asteriadi,⁴ C. N. Likos,³ F. Sciortino,¹ J. Roovers,⁵
H. Iatrou,⁶ N. Hadjichristidis,⁶ P. Tartaglia,⁷ H. Löwen,³ and D. Vlassopoulos^{4,8}

¹*Dipartimento di Fisica and CNR-INFM-SOFT, Università di Roma La Sapienza, I-00185 Rome, Italy*

²*ISC-CNR, Via dei Taurini 19, I-00185 Rome, Italy*

³*Institut für Theoretische Physik II, Heinrich-Heine-Universität, D-40225 Düsseldorf, Germany*

⁴*FO.R.T.H., Institute of Electronic Structure and Laser, GR-71110 Heraklion, Crete, Greece*

⁵*NRC, Institute for Chemical Process and Environmental Technology, Ottawa, Ontario, Canada*

⁶*University of Athens, Department of Chemistry, GR-15771 Athens, Greece*

⁷*Dipartimento di Fisica and CNR-INFM-SMC, Università di Roma La Sapienza, I-00185 Rome, Italy*

⁸*University of Crete, Department of Materials Science and Technology, GR-71003 Heraklion, Crete, Greece*

(Dated: November 23, 2018)

We examine the vitrification and melting of asymmetric star polymer mixtures by combining rheological measurements with mode coupling theory. We identify two types of glassy states, a *single* glass, in which the small component is fluid in the glassy matrix of the big one and a *double* glass, in which both components are vitrified. Addition of small star polymers leads to melting of *both* glasses and the melting curve has a non-monotonic dependence on the star-star size ratio. The phenomenon opens new ways for externally steering the rheological behavior of soft matter systems.

PACS numbers: 82.70.-y, 64.70.Pf, 83.80.Hj

The design of materials with well-defined rheological properties and the ability to alter these at wish, by tuning suitable control parameters of the system, are issues of central importance in today's soft matter research. Experimental findings, accumulating at a fast pace, call for the identification and profound understanding of the several underlying physical mechanisms that control the ability of soft materials to support stresses or flow under shear [1]. In several situations, e.g., in coating or processing applications, it is necessary to dramatically alter the viscoelastic properties of a material. One possibility to do so in a controlled way, is to exploit the phenomenon of dynamical arrest. Indeed, close to a liquid-glass transition, a small variation of external parameters produces a spectacular change in the elastic properties of the material without significantly affecting its structure [2].

Star polymers have emerged as an ideal model system for exploring the flow behavior of soft matter and elucidating its molecular origin. They consist of f polymer chains covalently anchored onto a common center [3]. Star polymer solutions are chemically simple, well-characterized and physically tunable in their softness, building thereby natural bridges between hard colloids and polymers. This property stems from the particular form of the effective, entropic interaction between star-polymer centers [4, 5], which has a logarithmic/Yukawa form at small/large separations. Technologically, star polymers are important in several applications such as their use as viscosity modifiers in the oil industry [3] or their novel applications as drug-delivery agents [6, 7].

In this work, we show how one can gain control over the rheological properties of soft, repulsive, glassy materials via the addition of a second, soft, repulsive component, which is chemically identical to the first but

smaller in size. We consider a star-polymer glass perturbed by smaller star-polymer additives. We observe melting of the big-star glass, induced by the small stars, and an unexpected non-monotonic dependence of the critical amount of additives, needed to melt the glass, on the big-small star size ratio. We also perform the corresponding calculations of the melting line, within the binary mode coupling theory (MCT) framework [8, 9]. The theoretical melting line is in agreement with the experimental one, reproducing the qualitative trends of the latter. We demonstrate that the non-monotonic behavior arises from two different mechanisms by which the presence of the additive significantly affects the rheological properties, depending on the size ratios between the components. The former rests on the fluidity of the smaller component in the *single glass* formed by the larger component. The latter stems from the mutual soft repulsions in the *double glass*, in which both components are vitrified. The melting of such a double glass represents a novel physical process, in which a glassy component is liquified through the addition of a second glassy component.

Binary mixtures of big and small (1,4-polybutadiene)-stars were prepared in toluene. Three different types of big stars were employed, having an average functionality $f_1 \cong 270$ arms and arm molecular weight M_a ranging from 18 000 to 42 000 g/mol [10]. Soft glasses were obtained at concentration $c_1/c_1^* \cong 1.4$, where c_1^* denotes the big-star overlap concentration. Additional measurements were also performed with big stars of functionality $f_1 = 128$ with arm molecular weight of about 80000 g/mol, which are very similar to the 270-stars [11]. We express the mixture composition by the values $\rho_1\sigma_1^3$ of the big and $\rho_2\sigma_1^3$ of the small stars, where ρ_i , $i = 1, 2$ are the respective number densities and σ_i

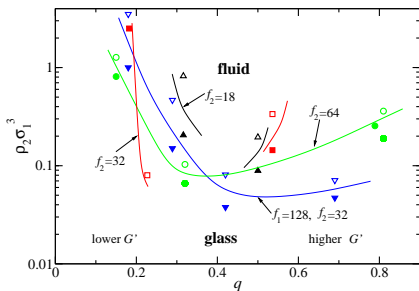


FIG. 1: Experimental kinetic ‘phase diagram’ of binary star mixtures, indicating regions of liquid and glass for different concentrations of added small star ρ_2 and size ratios q . Large stars of functionalities $f_1 = 270$ and 128 were used, with densities respectively $\rho_1 \sigma_1^3 = 0.345$ and 0.412 . Open symbols denote a liquid and closed ones a solid (glass) state. Only the data points closest to the melting lines are shown here. The lines through the data, passing above the full symbols and below the empty ones, are guides to the eye.

are the corona diameters of the big stars appearing in the effective interactions employed in the theory, coinciding with the stars’ hydrodynamic radii $R_{h,i}$, $i = 1, 2$. Small stars with three different functionalities, $f_2 = 16, 32$, and 64 , and molecular weights M_a between 1200 and $80\,000$ g/mol [12, 13, 14], were synthesized as well. Size ratios $q \equiv R_{h,2}/R_{h,1} = \sigma_2/\sigma_1$ varied from 0.15 to 1 . The mixture preparation protocol consisted of creating the big star glass at fixed number density $\rho_1 \sigma_1^3 = 0.345$ ($c_1/c_1^* = 1.4$) and then adding small stars with certain q at a desired density ρ_2 , under conditions of very gentle and prolonged stirring. In this procedure, the glass was broken and the mixture was left to ‘equilibrate’ again. For the $f_1 = 128$ -sample the fixed density was $\rho_1 \sigma_1^3 = 0.412$. Dynamical rheological measurements (time, strain and frequency sweeps) were carried out in order to identify the state of the particular samples (solid or liquid behaviour). A strain-controlled rheometer was utilized in the cone-and-plate geometry (25 mm diameter, 0.04 rad cone angle) and dynamic frequency sweep tests were conducted in the range $100 - 0.1$ rad/s at 20°C in the linear viscoelastic regime.

The experiments carried out provide evidence of U-shaped melting curves in the plane spanned by the size ratio q and the number density ρ_2 of the small additives, as well as quantitative distinctions of two types of glasses depending on the value of q . The glassy samples are characterized by the typical virtually frequency-independent elastic moduli G' ($350\text{ Pa} < G' < 800\text{ Pa}$) and respective weakly-frequency dependent viscous moduli G'' that exhibit a broad minimum ($G''_{\min} 20\text{ Pa} < G''_{\min} < 55\text{ Pa}$) [15]. For small concentration of small stars, the system exhibits moduli $G' > G''$ and $G' \sim \omega^0$, characteristic of solid, glass-like behavior [15, 16, 17]. As the density of the added small star increases, there is a dramatic change

in the mixture’s viscoelastic response. The glass melts, and a fluid results, whose moduli are weaker by orders of magnitude. A compilation of rheological results obtained from the available samples of different q and ρ_2 is presented in Fig. 1 for both studied functionalities of the large stars. In order to have a clear representation of all results in one plot, only the data closest to the glass-liquid boundaries are shown. This figure represents kinetic ‘phase diagrams’ of binary star mixtures, at fixed f_1 and ρ_1 and varying small-star characteristics in the (q, ρ_2) -parameter space. The results suggest that a U-shaped melting line separates the fluid (above) from the glass (below) states. This trend is general, since it is independent of the big stars used in the experiment.

Our theoretical analysis is based on a coarse-grained star description employing effective interactions [5] in binary star mixtures [18] with functionalities f_i and corona diameters σ_i , $i = 1, 2$, combined with mode coupling theory (MCT) [8, 9]. In the pure star solution, MCT predicts a glass line at large f above an f -dependent density [24], in agreement with experiment [2]. The equilibrium structure factors $S_{ij}(k)$, $k = 1, 2$, were calculated by solving the two-component Ornstein-Zernike equation [22] within the Rogers-Young closure [23]. The dynamics was calculated using two-component MCT [19, 20].

Upon addition of the smaller stars, the partial static structure factor $S_{11}(k)$ of the large ones shows a loss of structure, a phenomenon caused by the depletion-induced softening of the repulsions between the big stars. At the same time, the small-stars partial structure factor, $S_{22}(k)$, gradually develops growing peaks. These structural changes result into melting of the glass at a q - and f_2 -dependent density ρ_2^{melt} . Our theoretical results are summarized in Fig. 2, which can be interpreted as the theoretical ‘kinetic phase diagram’ of the system, in analogy with its experimental counterpart of Fig. 1. In agreement with experimental results, a characteristic U-shape is found for the melting curves at all studied f_2 . Above $q = 0.4$ for $f_2 = 64$, and $q = 0.45$ for $f_2 = 16$ and 32 , no melting is found for any density of the small stars.

The U-shape of the melting line points to the existence of two distinct microscopic melting mechanisms. For very small size of the additives, a standard depletion mechanism takes place. The osmotic pressure from the mobile, small stars, which are free to diffuse in the matrix formed by the big ones, leads to a reduction of the repulsive interactions between the latter. As a consequence, the cages that stabilize the glass are weakened, eventually breaking at a sufficiently high small-star concentration, at which the system melts. Since depletion is stronger at fixed ρ_2 as q grows, the melting curve has, in this regime, a negative slope in the (q, ρ_2) -plane, generating the left arm of the U-shaped line. However, as q further increases, the smaller stars become themselves slower and they begin to actively participate in the glass formation. At low additives concentration, the latter become trapped in the

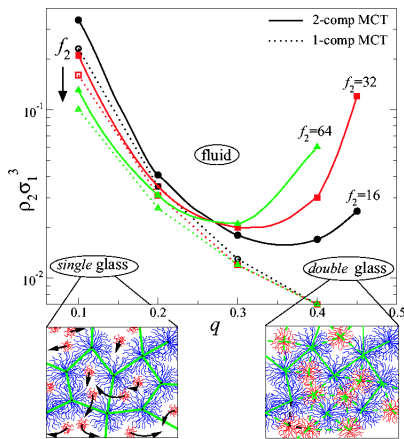


FIG. 2: Theoretical kinetic ‘phase diagram’ of binary star mixtures, calculated using MCT. The large-star functionality and concentration are fixed at the values $f_1 = 270$ and $\rho_1 \sigma_1^3 = 0.345$. The diagram is shown for three different functionalities f_2 of the small stars. Circles: $f_2 = 16$; squares: $f_2 = 32$; triangles: $f_2 = 64$. The lines going through the calculated points are guides to the eye. The cartoons display local arrangements in a single big-star glass with mobile small stars (left) and in a double glass in which there is mutual caging of both components (right).

voids left out of the glassy matrix. Hence, two competing mechanisms are at work: as before, the structure of the big stars is weakened by the addition of the small ones but, at the same time, the second component becomes increasingly glassy. The onset of this mechanism brings about a reversal of the slope of the melting curve, since now the tendency of the small stars to soften the repulsion between the big ones is counter-driven by their own opposing tendency to jam. As ρ_2 grows at fixed q , the small-star jamming cannot persist indefinitely, since the direct repulsions between the additives prevent them from occupying the same region of free space. As a result, melting of the glass takes place. We can distinguish between two different glassy states under the U-curve, one in which only the big stars are jammed (low q) and one in which both components are arrested (large q). We call the former *single-glass* and the latter *double-glass* state.

The above interpretation is supported, first, by a comparison with the results obtained if a one-component MCT-treatment is adopted, in which the smaller stars are assumed to form an ergodic fluid (dotted lines in Fig. 2). The two approaches yield very similar results at small size ratios, whereas the discrepancy becomes large at higher q 's, signaling the tendency of the small component to arrest. The deviation between the two approaches can also be understood in terms of the scaling of the short-time mobilities with size ratio [21]: as $q \rightarrow 1$ the time-scale separation between the two species disappears.

Further, we have calculated the elastic modulus G' fol-

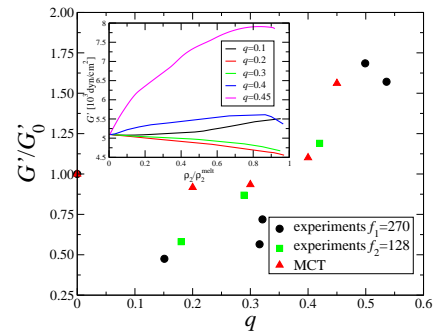


FIG. 3: Plot of the ratio G'/G'_0 , where G'_0 is the modulus of the system without additives, against size ratio q close to melting. Theory refers to the case $f_2 = 32$, while experiments refer to a compilation of several measured elastic moduli of star-star mixtures, obtained with different big and small stars at various concentrations of the additives. Inset: Dependence of the elastic modulus G' of the glass on ρ_2 ($f_2 = 32$).

lowing Ref. [25]. In the inset of Fig. 3 we show the theoretical results for G' , demonstrating that, for $q \leq 0.3$, G' has a maximum at $\rho_2 = 0$, whereas for the larger size ratio, $q = 0.4$, it has a minimum there. At small q , the additives lower G' through the softening of the big cages, whereas at high q they lead to stiffening of the glass through the fact that they are themselves driven to dynamical arrest. In Fig. 3, theoretical and experimental results for the *normalized* modulus G'/G'_0 are shown where $G'_0 \sim 500$ Pa stands for the average value of the elastic modulus of the big-star glass, without any additives. Experimental results display the same trends predicted theoretically. For small q , experimental values are much lower than the theoretical ones because MCT is not capable of taking into account the vast discrepancy in the mobilities of the two species in highly asymmetric mixtures. However, at larger q , in a full binary regime where the theory works best, the agreement between theory and experiments becomes almost quantitative.

Additional evidence for the fluidity of the small stars at low q -values and their jammed nature at high ones is offered by the calculated nonergodicity factor $f_{22}(k)$, shown in Fig. 4. Whereas the big-star nonergodicity factor $f_{11}(k)$ is rather insensitive to q , and remains roughly the same in all glassy states, $f_{22}(k)$ shows a dramatic change. For $q \leq 0.2$, $f_{22}(k)$ is very small and its nonzero values are confined to a very narrow, small k -domain. Such non-ergodicity factors are fully consistent with a mobile small component [26, 27, 28]. At high q -values $f_{22}(k)$ has the typical range of a fully arrested system.

The phenomenon of glass melting through polymer addition has been observed in hard-colloid-polymer (CP) mixtures [29, 30]. The physics and implications of this are, however, in our case very different. Whereas in the CP-case the solid melts due to the induction of short-range attractions on the colloids, which eventually drive

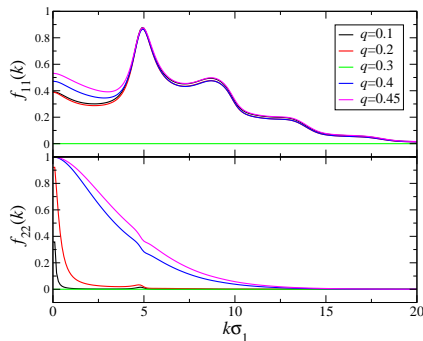


FIG. 4: The nonergodicity factors $f_{11}(k)$ (top) and $f_{22}(k)$ (bottom) of the two components, for $f_2 = 32$, $\rho_2\sigma_1^3 = 0.02$ at several q -values. For $q = 0.3$ the system is melted.

the formation of a reentrant, attractive glass, in our case effective attractions are completely absent. This fundamental difference is witnessed by the fact that in CP-mixtures melting takes place only for very asymmetric size ratios, $q \leq 0.1$, whereas in the present case it persists up to $q \cong 1$. The melting of the solid in CP-mixtures *requires* the fluidity of the added polymer [21]. To the contrary, for star mixtures, the addition of a second component that becomes increasingly *glassy* is capable of bringing about a melting of the double glass. This is made possible by the crucial role played by the softness of the interactions between all species, which allows for the and rearrangement of *soft* cages, a mechanism absent in CP-mixtures. In star-linear mixtures, only the left arm of the U-curve is seen experimentally, the melting phenomenon ceasing altogether at $q \cong 0.5$ [31]. There, the linear chains form a transient physical network, whereas stars are forced to maintain their spherical shape.

Our findings are general, since they are based on the softness of the effective interactions involved. A large class of composite soft materials, such as charge-stabilized colloidal dispersions, microgels, dendritic polymers or self-organized micelles are characterized by soft effective interactions. Charged suspensions and dusty plasmas, for instance, can be described by Yukawa potentials whose decay length and strength can be tuned by controlling the charges and the screening microions, in a similar way that the strength and range of the effective interactions between star polymers can be tuned by changing their functionality. Therefore, they should be amenable to manipulations of their rheology along the lines reported here. Functional versatility and viscosity control are desired material properties in medical, pharmaceutical and coating applications as well. Controlling these products near vitrification transitions, provides a means to achieve the desired properties variation.

We thank E. Stiakakis for assistance with some measurements. This work has been supported by MIUR

FIRB, MRTN-CT-2003-504712, by the DFG within the SFB-TR6, and by the EU within the NoE “Softcomp”. C.M. thanks the Düsseldorf Entrepreneurs Foundation for a Ph.D. Fellowship.

-
- [1] *Soft and Fragile Matter: Nonequilibrium Dynamics, Metastability and Flow*, ed. by M. E. Cates and M. R. Evans, Scottish Graduate Series, Vol. 53 (IOP Publishing, Bristol, 2000).
 - [2] D. Vlassopoulos, *J. Polym. Sci. Part B: Polym. Phys.* **42**, 2931 (2004).
 - [3] G. S. Grest *et al.*, *Adv. Chem. Phys.* **XCIV**, 67 (1996).
 - [4] T. A. Witten, and P. A. Pincus, *Macromolecules* **19**, 2509 (1986).
 - [5] C. N. Likos *et al.*, *Phys. Rev. Lett.* **80**, 4450 (1998).
 - [6] J. Djordjevic *et al.* *AAPS Pharmsci.* **5**, Art. No. 26 (2003).
 - [7] H. Yang and S. T. Lopina, *J. Biomat. Sci.-Polym. E.* **14**, 1043 (2003).
 - [8] W. Götze, in *Liquids, Freezing and Glass Transition*, p.287, J.-P. Hansen, D. Levesque, and J. Zinn-Justin (eds.), North Holland, Amsterdam (1991).
 - [9] W. Götze, *J. Phys.: Condens. Matter* **11**, A1 (1999).
 - [10] J. Roovers *et al.*, *Macromolecules* **22**, 1897 (1989).
 - [11] D. Vlassopoulos *et al.*, *J. Phys.: Condens. Matter* **13**, R855 (2001).
 - [12] P. M. Toporowski and J. Roovers, *J. Polym. Sci.: Part A: Polym. Chem. Ed.* **24**, 3009 (1986).
 - [13] L.-L. Zhou *et al.*, *Rubber Chem. Technol.* **65**, 303 (1992).
 - [14] J. Roovers *et al.*, *Macromolecules* **26**, 4324 (1993).
 - [15] T. G. Mason and D. A. Weitz, *Phys. Rev. Lett.* **75**, 2770 (1995).
 - [16] R. G. Larson, *The Structure and Rheology of Complex Fluids* (Oxford, New York, 1999).
 - [17] L. Raynaud, *et al.*, *J. Colloid Interf. Sci.* **181**, 11 (1996).
 - [18] C. von Ferber *et al.*, *Phys. Rev. E* **62**, 6949 (2000).
 - [19] Götze, W. in *Amorphous and Liquid Materials*, p. 34, Vol. 118 of *NATO Advanced Study Institute, Series E: Applied Sciences*, edited by E. Lüscher, G. Fritsch, and G. Jacucci Nijhoff, Dordrecht, (1987).
 - [20] J.-L. Barrat and A. Latz, *J. Phys.: Condens. Matter* **2**, 4289 (1990).
 - [21] E. Zaccarelli *et al.*, *Phys. Rev. Lett.* **92**, 225703 (2004).
 - [22] J.-P. Hansen and I. R. McDonald, *Theory of Simple Liquids*, 2nd ed., Academic, London, (1986).
 - [23] F. A. Rogers and D. A. Young, *Phys. Rev. A* **30**, 999 (1984).
 - [24] G. Foffi *et al.*, *Phys. Rev. Lett.* **90**, 238301 (2003).
 - [25] G. Nägele and J. Bergenholtz, *J. Chem. Phys.* **108**, 9893 (1998).
 - [26] J. S. Thakur and J. Bosse, *Phys. Rev. A* **43**, 4378 (1991).
 - [27] J. S. Thakur and J. Bosse, *Phys. Rev. A* **43**, 4388 (1991).
 - [28] J. Bosse and Y. Kaneko, *Phys. Rev. Lett.* **74**, 4023 (1995).
 - [29] K. N. Pham, *et al.* *Science* **296**, 104–106 (2002).
 - [30] T. Eckert and E. Bartsch, *Phys. Rev. Lett* **89**, 125701 (2002).
 - [31] E. Stiakakis *et al.*, *Phys. Rev. Lett.* **89**, 208302 (2002).